SUPPLEMENT

ANALOGIES OF OCEAN/ ATMOSPHERE ROTATING FLUID DYNAMICS WITH GYROSCOPES
Teaching Opportunities

BY THOMAS W. N. HAINE AND DEEPAK A. CHERIAN

Here we provide a mathematical analysis of gyroscope dynamics, concentrating on precession and nutation. Useful references on this topic include Goldstein (1981) and Hasbun (2009). We then make the connection to the shallow-water dynamics of a thin fluid layer in a rotating frame (see, e.g., see Gill 1982; Vallis 2006). Table S1 summarizes the main results.

GYROSCOPE ENERGETICS AND LAGRANGIAN.
The gyroscope has one axis of symmetry, its spindle, which has moment of inertia I_3 and is also one of the principal axes of the gyroscope $z^\star$. As one point of the gyroscope is fixed (the center of mass for the gimballed device considered here, which defines the origin), the motion can be completely specified by the three Euler angles θ, ϕ, ψ (Fig. S1). They are as follows:

(i) θ, the inclination of the $z^\star$ axis from the vertical axis z;
(ii) ϕ, the rotation angle of the gyroscope about the vertical axis z, specifically the angle between the x axis and the line defined by the intersection of the (x, y) and $(x^\star, y^\star)$ planes (the line of nodes); and

(iii) ψ, the rotation angle of the gyroscope about the $z^\star$ axis, specifically the angle between the line of nodes and the $x^\star$ axis.

To transform from inertial (x, y, z) to body $(x^\star, y^\star, z^\star)$ axes when they initially coincide, we compose the following steps: First rotate ϕ about z, next rotate θ about the axis defined by the present position of $x^\star$, and finally rotate ψ about $z^\star$ (this sequence is called the ZX'Z″ convention). Notice that precession of the gyroscope is $\dot{\phi}$, and nutation involves both $\dot{\phi}$ and $\dot{\theta}$ in quadrature. It may help to remember that ϕ is equivalent to longitude, and θ is equivalent to colatitude (90° – latitude). Other conventions to measure the orientation of the two frames exist: for instance, the "yaw, pitch, roll" angles used to describe spacecraft attitude.

Using the body frame, we can easily compute the kinetic energy, the Lagrangian, and the total energy of the motion. This task requires the angular velocities $(\omega_1, \omega_2, \omega_3)$ about the $(x^\star, y^\star, z^\star)$ axes, respectively, which can be written in terms of the Euler angles as

$$\omega_1 = \dot{\phi} \sin \theta \sin \psi + \dot{\theta} \cos \psi, \qquad \text{(S1)}$$

TABLE S1. Similarities and differences between rotating shallow-water flow with vanishing wavenumber (hence no spatial variations) and the gyroscope. See the text for details (the appropriate sections are indicated). See also Table 1 of the main text.

Similarities:	Rotating shallow-water flow	Gyroscope
Low-frequency forced motion and minimum energy state	Geostrophic flow	Precession
High-frequency free motion	Inertial oscillation	Nutation
Nondimensional number measuring rotational effects ("why the gyroscope does not topple" and "link to the shallow-water equations")	Rossby number, $$\mathrm{Ro} = \frac{(v_\lambda^2 + v_\phi^2)^{1/2}}{\Omega L}$$	Gyroscope number, $$\varepsilon = \frac{I\omega_{pe}}{I_3\omega_3}$$
Unforced dynamics ("equations of motion: precession and nutation" and "link to the shallow-water equations")	$$\dot{v}_\lambda - (v_\lambda v_{\phi'}/r)\tan\phi' - 2\Omega\sin\phi' v_{\phi'} = 0$$ $$\dot{v}_{\phi'} + (v_\lambda^2/r)\tan\phi' + 2\Omega\sin\phi' v_\lambda = 0$$	$$I\ddot{\theta} - I\dot{\phi}^2\sin\theta\cos\theta + I_3\omega_3\dot{\phi}\sin\theta = 0$$ $$I\ddot{\phi}\sin\theta + 2I\dot{\theta}\dot{\phi}\cos\theta - I_3\omega_3\dot{\theta} = 0$$
Small-amplitude dynamics ("equations of motion: precession and nutation" and "link to the shallow-water equations")	$$\dot{u} - fv = M$$ $$\dot{v} + fu = 0$$	$$\ddot{\theta} + \omega_n\dot{\phi}\sin\theta_0 = \omega_p\omega_n\sin\theta_0$$ $$\ddot{\phi}\sin\theta_0 - \omega_n\dot{\theta} = 0$$
Unforced Lagrangian ("gyroscope energetics and Lagrangian" and "link to the shallow-water equations")	$$L_p = \frac{r^2}{2}[\dot{\phi}'^2 + \dot{\lambda}^2\cos^2\phi' + 2\Omega\dot{\lambda}\cos^2\phi']$$	$$L_g = \frac{I}{2}\left[\dot{\theta}^2 + \dot{\phi}^2\left(\sin^2\theta + \frac{I_3}{I}\cos^2\theta\right)\right]$$ $$+ \frac{I_3}{2}[2\dot{\phi}\dot{\psi}\cos\theta + \dot{\psi}^2]$$
Differences:		
Form of Coriolis term ("link to the shallow-water equations")	Clockwise inertial circles in northern hemisphere, beta effect	Anticlockwise nutation, no analog to beta effect

$$\omega_2 = \dot{\phi}\sin\theta\cos\psi - \dot{\theta}\sin\psi, \text{ and} \quad (S2)$$

$$\omega_3 = \dot{\phi}\cos\theta + \dot{\psi}, \quad (S3)$$

(see Goldstein 1981, p. 176). The kinetic energy is therefore

$$T = \frac{I}{2}(\omega_1^2 + \omega_2^2) + \frac{I_3}{2}\omega_3^2 \quad (S4)$$

$$= \frac{I}{2}(\dot{\theta}^2 + \dot{\phi}^2\sin^2\theta) + \frac{I_3}{2}(\dot{\psi} + \dot{\phi}\cos\theta)^2, \quad (S5)$$

where I is the moment of inertia of the gyroscope about any axis through the origin that is perpendicular to the symmetry axis. The potential energy is given by

$$V = mgl\cos\theta, \quad (S6)$$

for applied mass m, at a distance l from the origin.

The Lagrangian, $L_g = T - V$, is therefore

$$L_g = \frac{I}{2}(\dot{\theta}^2 + \dot{\phi}^2\sin^2\theta) + \frac{I_3}{2}(\dot{\psi} + \dot{\phi}\cos\theta)^2 \quad (S7)$$
$$- mgl\cos\theta.$$

This formula does not explicitly include ϕ or ψ and the corresponding momenta are constants of the motion

$$p_\psi = \frac{\partial L_g}{\partial\dot{\psi}} = I_3(\dot{\psi} + \dot{\phi}\cos\theta) = I_3\omega_3 \equiv Ia, \text{ and} \quad (S8)$$

$$p_\phi = \frac{\partial L_g}{\partial\dot{\phi}} = I\sin^2\theta\dot{\phi} + I_3\omega_3\cos\theta \equiv Ib. \quad (S9)$$

Angular momentum about these axes p_ϕ, p_ψ is therefore conserved. In particular, ω_3, the gyroscope's spin about its axis of symmetry z^*, and the angular momentum about the vertical axis z are constant. Physically, we know that the gravitational torque is applied along the line of nodes, perpendicular to both z and z^*. Hence,

it cannot change angular momentum in any direction lying in the plane spanned by z and z^*.

ENERGY ANALYSIS OF PRECESSION AND NUTATION.

Rearranging (S8) and (S9) gives

$$\dot{\phi} = \frac{b - a\cos\theta}{\sin^2\theta}, \text{ and} \qquad (S10)$$

$$\dot{\psi} = \frac{Ia}{I_3} - \cos\theta\left(\frac{b - a\cos\theta}{\sin^2\theta}\right). \qquad (S11)$$

Using these relations, the (conserved) total energy of the system may be expressed as

$$E = T + V, \qquad (S12)$$

$$= \frac{I}{2}(\dot{\theta}^2 + \dot{\phi}^2\sin^2\theta) + \frac{I_3}{2}(\dot{\psi} + \dot{\phi}\cos\theta)^2 \qquad (S13)$$
$$+ mgl\cos\theta,$$

$$= \frac{I}{2}\dot{\theta}^2 + \frac{I}{2}\frac{(b - a\cos\theta)^2}{\sin^2\theta} + \frac{I_3}{2}\omega_3^2 + mgl\cos\theta. \qquad (S14)$$

As ω_3 is a constant [from (S8)] the expression $E - \frac{I_3}{2}\omega_3^2$ may be considered an effective energy in θ only. The expression may be interpreted as the sum of an effective kinetic energy $\frac{I}{2}\dot{\theta}^2$ and an effective potential,

$$V'(\theta) = mgl\cos\theta + \frac{I}{2}\left(\frac{b - a\cos\theta}{\sin\theta}\right)^2 \qquad (S15)$$

(the prime is not a derivative).

The plot of $V'(\theta)$ against θ shows a potential well. For example, Fig. S2 shows the effective potential for the MITAC gyroscope shown in Figs. 5 and 7 of the main text. The gravitational contribution to V' [first term on right of (S15)] decreases with increasing angle θ. It is dominated by the rotational contribution to V', however [second term in (S15)]. The total energy of the system is fixed by the initial conditions and remains constant. Kinetic energy $\frac{I}{2}\dot{\theta}^2$ is therefore traded for potential energy and the system oscillates between two values of θ. In Fig. S2 the initial θ is $\pi/2$ and the initial $\dot{\phi}$ is zero. The minimum of V' lies at higher θ and the motion involves nutation with θ

oscillating between the two values whose V' vanishes, as shown in the inset. Hence, the gyroscope symmetry axis oscillates between the two extreme values of θ (nutation) while simultaneously moving with an angular velocity $\dot{\phi}$ about the z axis (precession plus nutation).

WHY THE GYROSCOPE DOES NOT TOPPLE.

This potential well analysis also illuminates the common question of why a gyroscope does not topple over. To see this, compute the extreme values of θ for the motion. Here, $\theta = \pi/2$, $\dot{\phi} = 0$ at the initial time. Thus, $a = (I_3\omega_3)/I$, $b = 0$, and the extreme values are $\pi/2$ (the initial angle) and a root of

$$\cos^2\theta - \frac{I_3^2\omega_3^2}{2Imgl}\cos\theta - 1 = 0. \qquad (S16)$$

This other root is approximately $\pi/2 + 2Imgl/(I_3^2\omega_3^2)$ for the case of rapid rotation. The MITAC gyroscope is in this regime and we find that the second root is around $\pi/2 + 0.0058$, in good agreement with Fig. S2. Now note that the intrinsic frequency of the simple pendulum in this system is

$$\omega_{pe} = \sqrt{\frac{mgl}{I}} \quad \text{(pendulum frequency)}, \qquad (S17)$$

which suggests the nondimensional ratio of angular momenta, $\varepsilon = \frac{I\omega_{pe}}{I_3\omega_3}$, as a useful parameter for the system [ε is similar but distinct from the "fast top" limit that Goldstein (1981) discusses]. For the case considered here, the nutation therefore oscillates between $\theta = \pi/2$ and the appropriate root of

z

z^* θ

x^* y^*

ψ line of nodes

x

ϕ y

(x, y, z) space axes
(x^*, y^*, z^*) body axes
(θ, ϕ, ψ) Euler angles
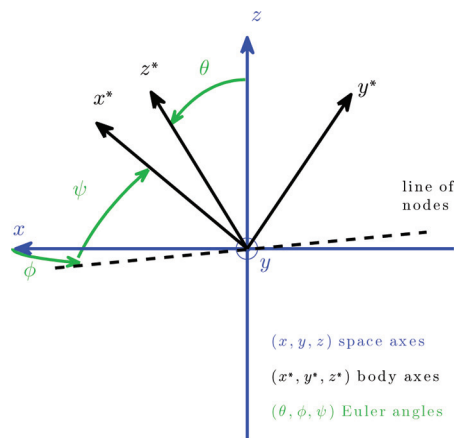
FIG. S1. (left) Coordinate system for the gyroscope. Space axes in the inertial frame are (x, y, z); axes in the body frame are (x^*, y^*, z^*); and Euler angles that relate the two systems are θ, ϕ, ψ. The intersection of the (x, y) and (x^*, y^*) planes is the line of nodes. (right) In the gyroscope shown in the photograph, z^* is along the spin axis and the line of nodes is the axis of the outer semicircular gimbal ring.

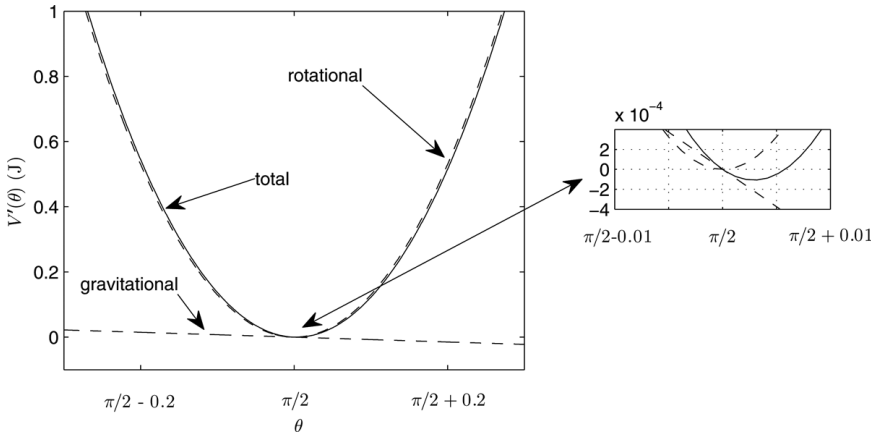**FIG. S2. Potential well for the MITAC gyroscope shown in Figs. 5 and 7 of the main text. The solid line is the total energy, which is the sum of the gravitational and rotational energies (dashed). See (S15) and text for details.**

$$\cos^2 \theta - \frac{1}{2\varepsilon^2} \cos \theta - 1 = 0. \qquad \text{(S18)}$$

The parameter ε measures the relative importance of the gravitational forces to the gyroscopic forces in the system, analogous to the Rossby number in rotating fluid dynamics (see below). For the MITAC case $\varepsilon = 0.0538$, indicating the strong influence of gyroscopic forces and a small θ range for nutation. Figure S3 shows the general case for wide-ranging ε. Small ε, like the MITAC gyroscope, corresponds to a small angular range of nutation and hence almost no topple. Large ε corresponds to a large angular range: the gyroscope topples over and resembles a pendulum. The definition of the Euler angles means that θ can never exceed π. Strictly, it can only equal π for vanishing ω_3, but in practice the trajectory for very small ω_3 looks like a swinging pendulum rather than a nutating gyroscope. The ratio of angular momenta ε controls this transition.

EQUATIONS OF MOTION: PRECESSION AND NUTATION. This analysis easily leads to the equations of motion for a gyroscope. The Lagrange equation $(d/dt)(\partial L/(\partial \dot{q}) - \partial L/\partial q = 0$ for the coordinate $q = \theta$ gives

$$I\ddot{\theta} = I\dot{\phi}^2 \sin \theta \cos \theta + (mgl - I_3 \omega_3 \dot{\phi}) \sin \theta \qquad \text{(S19)}$$

(angular momentum about the line of nodes is not constant in general) while (S9) yields

$$I\ddot{\phi} \sin \theta = -2I\dot{\theta}\dot{\phi} \cos \theta + I_3 \omega_3 \dot{\theta}. \qquad \text{(S20)}$$

As demonstrated below, these equations are very closely related to the equations governing flow on a

rotating sphere of a shallow fluid with no spatial variations or equivalently the motion of a frictionless particle on a rotating sphere. Analytic solutions to these equations exist based on solving (S14) for θ, although they involve elliptic integrals (Goldstein 1981, p. 216).

For slow precession and rapid rotation (small ε), these expressions can be linearized to yield [Eqs. (6a) and (6b) of the main text]

$$\ddot{\theta} = (\omega_p \omega_n - \omega_n \dot{\phi}) \sin \theta_0 \qquad \text{(S21)}$$

$$\ddot{\phi} \sin \theta_0 = \omega_n \dot{\theta}, \qquad \text{(S22)}$$

where precession frequency ω_p and nutation frequency ω_n are

$$\omega_p = \frac{mgl}{I_3 \omega_3} = \varepsilon \omega_{pe} \quad \text{(precession frequency)} \qquad \text{(S23)}$$
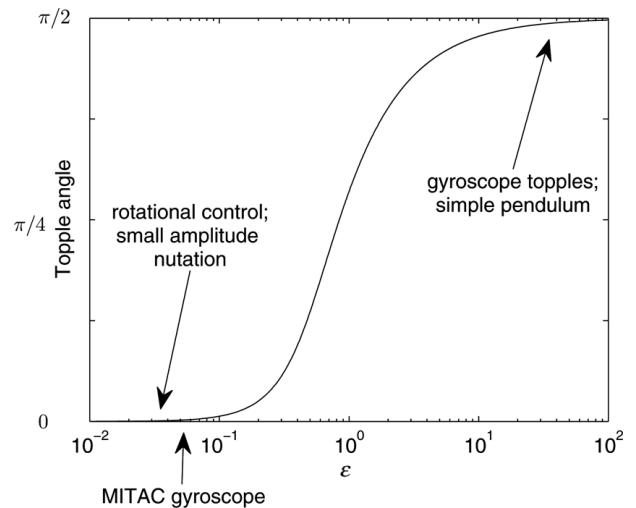
and

FIG. S3. Gyroscope transition from rotational control with small nutation to toppling like a simple pendulum. The topple angle (the maximum θ angular range) is shown as a function of $\varepsilon = \frac{I\omega_{pe}}{I_3\omega_3}$ for the case of a gyroscope initially at rest with $\theta = \pi/2$. See text for details.

$$\omega_n = \frac{I_3 \omega_3}{I} = \frac{\omega_{pe}}{\varepsilon} = a \quad \text{(nutation frequency)} \quad \text{(S24)}$$

and θ_0 is the angle of the gyroscope symmetry axis from the vertical, which well approximates $\theta(t)$ by virtue of the small nutation amplitude explained above.

The general solution in this case is

$$\dot{\phi} = \Re\{Ae^{i\omega_n t} + \omega_p\} \quad \text{(S25)}$$

and

$$\dot{\theta} = \Re\{Ai \sin\theta_o e^{i\omega_n t}\}, \quad \text{(S26)}$$

for constant A. The motion consists of a superposition of slow precession (gyroscope tip traces out a horizontal circle at rate ω_p) and rapid nutation (tip traces out a circle at rate ω_n). The ratio of the periods of these oscillations is ε^{-2} [from (S23) and (S24)], which for the MITAC gyroscope in Figs. 5 and 7 of the main text is 345.

LINK TO THE SHALLOW-WATER EQUATIONS.

It is revealing to consider the equations satisfied by a frictionless particle sliding on a sphere of radius r in a frame rotating at rate Ω. They are

$$\frac{dv_\lambda}{dt} - \frac{v_\lambda v_{\phi'}}{r}\tan\phi' - 2\Omega\sin\phi' v_{\phi'} = 0 \quad \text{(S27)}$$

and

$$\frac{dv_{\phi'}}{dt} + \frac{v_\lambda^2}{r}\tan\phi' + 2\Omega\sin\phi' v_\lambda = 0, \quad \text{(S28)}$$

where $v_\lambda = \dot{\lambda} r \cos\phi'$ and $v_{\phi'} = \dot{\phi}'r$ are the velocity components in the zonal and meridional directions, respectively, for longitude λ and latitude ϕ measured in the rotating frame (Ripa 1997). These equations coincide with the shallow-water equations on a rotating sphere where spatial variations are ignored (Gill 1982).[1] Rewriting these equations in a more obvious form, we have

$$\ddot{\lambda}\cos\phi' = 2\dot{\lambda}\dot{\phi}'\sin\phi' + 2\Omega\dot{\phi}'\sin\phi' \quad \text{(S29)}$$

and

$$\ddot{\phi}' = -\dot{\lambda}^2\sin\phi'\cos\phi' - 2\Omega\dot{\lambda}\sin\phi'\cos\phi', \quad \text{(S30)}$$

which describe the (λ, ϕ') position of a particle moving in the flow. These formulas should be compared to (S19) and (S20). The two sets are similar, and substitution of

$$(\phi', \lambda, 2\Omega) \Leftrightarrow (\pi/2 - \theta, \phi, I_3\omega_3/I) \quad \text{(S31)}$$

to yield

$$I\ddot{\theta} = I\dot{\phi}^2\sin\theta\cos\theta + I_3\omega_3\dot{\phi}\sin\theta\cos\theta \quad \text{(S32)}$$

and

$$I\ddot{\phi}\sin\theta = -2I\dot{\theta}\dot{\phi}\cos\theta - I_3\omega_3\dot{\theta}\cos\theta \quad \text{(S33)}$$

makes them nearly coincide.

Two slight differences remain. First, the torque term proportional to mgl is missing from the shallow-water system. This discrepancy is cosmetic, however: the dynamical response to a momentum source in the shallow-water system is well known. A constant momentum source can be added to (S27) and (S28) and this makes most sense on the f plane, as discussed below. Second, the term in the gyroscope angular momentum about its symmetry axis, $I_3\omega_3$, is missing a minus $\cos\theta$ factor in (S19) and (S20). This factor is present in the shallow-water system, however, because the Coriolis force varies with latitude as $\sin\phi'$. For large angular excursions [where the Rossby number

$$\text{Ro} = \left(\sqrt{v_\lambda^2 + +v_\phi^2}\right)/\Omega r,$$

is large], this dependence causes particles to cross the equator and execute figure-eight trajectories between hemispheres. Particles also drift zonally, at an average rate $\langle\dot{\lambda}\rangle = -(1/2r)\beta R^2 \sec\theta_0$ for small excursions about latitude θ_0. In this expression the inertial oscillation radius is $R = (r/2)\text{Ro} \csc\theta_0$ and $\beta = (2\Omega/r)\cos\theta_0$ represents the beta effect due to latitudinal variation of the Coriolis parameter (Ripa 1997). No such westward drift occurs in the nutating gyroscope, which lacks an equivalent to the beta effect. The sign difference in the Coriolis term between the two systems simply means that the gyroscope axis is deflected in the opposite direction to the deflection of a particle by the Coriolis force: nutation traces out anticlockwise loops in (ϕ, θ), whereas inertial oscillations are clockwise (as seen in Figs. 2 and 4 of the main text). In the Southern Hemisphere the sign difference disappears.

---

[1] Note that the linearized shallow-water equations on a rotating sphere, the Laplace tidal equations, present an eigenvalue problem for the quantized modes (Longuet-Higgins 1968). The eigenfunctions have non-vanishing spatial structure, however. For this reason, (S27) and (S28) strictly apply to a discrete particle on a rotating sphere, not global fields of shallow fluid flow. This technical distinction does not undermine the heuristic physical links between the gyroscope and the shallow-water system.

Just as for the gyroscope equations, analytic solutions exist for (S32) and (S33) [or (S27) and (S28)]. The presence of the minus $\cos \theta$ factor changes the details slightly, but the basic strategy in terms of elliptic integrals still applies (Whipple 1917). The analytic solutions may be useful for testing numerical algorithms to solve the shallow-water equations on a sphere.

Unsurprisingly, the equations for particle motion on a rotating sphere (S27) and (S28) can also be derived from a Lagrangian: namely,

$$L_p = \frac{r^2}{2}\left[(\dot{\lambda} + \Omega)^2 \cos^2 \phi' + \dot{\phi}'^2 - \Omega^2 \cos^2 \phi' \right] \quad (S34)$$

(Ripa 1997). Absence of λ and t from L_p means the system conserves total angular momentum about the axis of rotation $r^2\cos^2\phi'(\dot{\lambda} + \Omega)$ and energy $(1/2)(v_\lambda^2 + v_\phi^2)$, respectively. Comparison of (S34) with (S7) is revealing: the dependence on $\dot{\phi}' \Leftrightarrow -\dot{\theta}$ coincides and the dependence on $\dot{\lambda} \Leftrightarrow \dot{\phi}$ coincides too, apart from a difference in a trigonometric prefactor. The particle system has no equivalent to the Euler angle ψ or the torque-generating mass m, however. The two Lagrangians exactly coincide for vanishing gyroscope I_3 and m when the sliding particle is observed in an inertial frame $\Omega = 0$. Table S1 shows L_g and L_p written in their most similar forms.

For small (ϕ, θ) excursions (small Ro), the unbounded (or periodic) midlatitude f plane is a very useful and well-known local approximation to the sphere (Gill 1982; Vallis 2006). The quadratic metric terms then vanish from (S27) and (S28) and we have the familiar Cartesian system with negligible beta effect [Eqs. (5a) and (5b) of the main text]:

$$\frac{du}{dt} - fv = M \quad (S35)$$

and

$$\frac{dv}{dt} + fu = 0, \quad (S36)$$

for zonal and meridional currents $u = v_\lambda$, $v = v_{\phi'}$ and constant $f = 2\Omega \sin \theta_0$. This system almost exactly coincides with the gyroscope system under the same approximation (i.e., of rapid primary spin and therefore small ε). A momentum source M on the right-hand side of (S35), for example, is now physically reasonable. It corresponds to a pressure gradient imposed at large scales and leads to geostrophic flow $v_g = -M/f$, akin to precession, superimposed on inertial oscillations. Substitution of

$$(u, v, f, M) \Leftrightarrow (\dot{\theta}, \dot{\phi}, -\omega_n, \omega_p\omega_n) \quad (S37)$$

yields (S21) and (S22) for $\theta_0 = \pm\pi/2$ (the poles). For more general θ_0, the two systems are slightly different. Gyroscopic nutation traces ellipses in (ϕ, θ) space (circles in physical space), whereas inertial oscillation trajectories are circular in the Cartesian geometry. This correspondence between the gyroscope equations and the shallow-water equations (specifically, the equations for a particle on a rotating sphere) exhibits the mathematical isomorphism between the two physical systems.

REFERENCES

Gill, A. E., 1982: *Atmosphere–Ocean Dynamics.* Academic Press, San Diego.

Goldstein, H., 1981: *Classical Mechanics.* 2nd ed., Addison-Wesley, 672 pp.

Hasbun, J. E., 2009: *Classical Mechanics with MATLAB Applications.* 1st ed. Jones and Bartlett, 548 pp.

Longuet-Higgins, M. S., 1968: The eigenfunctions of Laplace's tidal equations over a sphere. *Philos. Trans. Roy. Soc. London*, **262A**, 511–607.

Ripa, P., 1997: "Inertial" oscillations and the β-plane approximation(s). *J. Phys. Oceanogr., 27,* 633–647.

Vallis, G. K., 2006: *Atmospheric and Oceanic Fluid Dynamics: Fundamentals and Large-Scale Circulation.* 1st ed., Cambridge University Press, 745 pp.

Whipple, F. J. W., 1917: The motion of a particle on the surface of a smooth rotating globe. *London Edinburgh Philos. Mag. J. Sci., 33,* 457–471.